Journal of Applied Electrochemistry **32**: 1371–1378, 2002.

Mechanism of copper electrodeposition by pulse current and its relation to current efficiency

W-C. TSAI, C-C. WAN* and Y-Y. WANG
Department of Chemical Engineering, National Tsing-Hwa University, Hsinchu, Taiwan 300
*(*author for correspondence, fax: +886 3 5715408, e-mail: ccwan@mx.nthu.edu.tw)*

Received 19 April 2002; accepted in revised form 6 September 2002

Key words: copper electrodeposition, current efficiency, electrode kinetics, overpotential response, pulse plating

Abstract

The effects of pulse periods and duty cycles on the current efficiency of acid copper plating in a wide range of pulse periods from 200 to 0.02 ms were studied. It was found the current efficiency decreased with shortening pulses in the millisecond range but increased with shortening pulses in the microsecond range. A mathematical model based on the concept of equivalent circuit was employed to simulate the potential responses. Shortening the pulse period was found to change the rate-determining step from charge transfer and surface diffusion to the first step charge transfer. In the millisecond range, the current efficiency decreases with shortening pulse period due to the disproportionation of cuprous ions and the dissolution of copper adatom. However, in the microsecond range, the current efficiency was found to increase with decreasing pulse period because the adatoms are directly incorporated into steps and kink sites, and the disproportionation of cuprous ions or the dissolution of copper adatoms has less chance to occur.

List of symbols

C_{dl}	capacitance of double layer (μF cm^{-2})
C_{psd}	pseudocapacitance (μF cm^{-2})
E	electrode potential (V)
E_{eq}	equilibrium potential between the working and the reference electrode (V)
i_C	capacitive current density (A cm^{-2})
i_F	faradaic current density (A cm^{-2})
i_p	pulse current density (A cm^{-2})
p	pulse number
R_{ct}	resistance of the first-step charge transfer (Ω cm^2)
R_{sd}	resistance of the second-step charge transfer and surface diffusion (Ω cm^2)
R_{sol}	resistance of the electrolytic solution (Ω cm^2)
t	time (s)
t_{off}	off-time (s)
t_{on}	on-time (s)
t_p	pulse period (s)
η	surface overpotential (V)
η^I	potential drop corresponding to the first-step charge transfer (V)
η^{II}	potential drop corresponding to the second-step charge transfer and surface diffusion (V)

1. Introduction

Pulse plating can enhance mass transfer and affect deposit properties including morphology, porosity, hardness and crystal orientation by adjusting the on-time (t_{on}), off-time (t_{off}) and pulse current density (i_p). This method is widely used in the plating industries, including the IC and PCB industries [1–5].

Extensive theoretical work has been done on the mass transfer of pulse plating [6–9]. In principle, the on-time should be as short as possible and the off-time should be as long as possible. However, Wan et al. [10, 11] found that the cathodic current efficiency of copper in pulse plating decreases with decreasing t_{on} in the millisecond range. Similar results were shown by Chen and Wan [12] in the pulse plating of acidic lead–tin alloy, tin, lead and copper systems. A mechanism of electrodeposition was formulated to explain why current efficiency decreases under pulse current conditions, proposing that the lowering of current efficiency was caused by the disproportionation of cuprous ions and the dissolution of adatoms.

The current efficiencies of many other metal have also been studied in the millisecond range. Eckler et al. [13] found that for the pulse plating of chromium–molybdenum alloy, the current efficiency had a minimum with t_{on} ranging from 100 to 0.1 ms. Pulse waveforms of 3 ms t_{on} and 3 ms t_{off} were recommended. Yoshimura et al. [14] studied the pulse of palladium and found that the current efficiency decreased with decreasing t_{on} in the range from 10 to 0.1 ms. Current efficiencies of metal deposition in the microsecond range have also been studied. Hosokawa et al. [15] concluded that the current efficiency for rhenium plating exhibited a sharp

Table 1. Effect of N_2 purge and bath composition on current efficiency under direct current

Plating baths/M		N_2 purge	Temp. /°C	Current density /mA cm^{-2}	Current efficiency /%		Average
$CuSO_4 \cdot 5H_2O$	H_2SO_4						
0.384	2.06	none	room	7.96	132.4	114.3	123.4
0.2	0.45	2 h	25	7.89	99.1	98.8	99.0

maximum in the range of t_{on} from 1 ms to 1 μs. Miu and Fung [16] found that microsecond pulses could improve current efficiency, increase hardness and reduce porosity and contact resistance of rhodium deposits. However, so far no satisfactory explanation has been provided for those seemingly inconsistent findings in the millisecond and microsecond pulse plating.

The pulse current is also influenced by the double layer of the electrode, especially for very short pulses. Puippe and Ibl [17] postulated a model to describe the mass transfer and the double layer effect in pulse plating. According to their model, charging and discharging the double layer would distort the pulse current waveform when the pulse period is very short. Our previous study showed that the overpotential response of pulse current was significantly affected by the double layer in the millisecond range [18]. However, the relation between current efficiency and double layer effect is still missing.

Since electrodeposition using microsecond pulses is different from that using millisecond pulses, we carried out a systematic study on the effect of pulse periods and duty cycles on the current efficiency over a wide range of pulse periods covering from 200 to 0.02 ms. A mathematical model based on the concept of equivalent circuit, which includes the double effect, has also been developed to simulate the overpotential response in pulse plating. As a result, the change of current efficiency from microsecond to millisecond range can be predicted from a single model.

2. Experimental details

A three-electrode glass cell was used with a copper plate (1.5 cm × 3 cm) as the counter anode and a copper wire as the reference electrode. The working cathode, (kept motionless) was a copper disc 1.27 cm in diameter. The reference electrode was placed close to the working electrode to reduce the ohmic overpotential. Prior to electrodeposition, the electrode surface was carefully polished with fine emery paper, and then rinsed with deionized water. The current efficiency was calculated by the gravimetric method. The working electrode was rinsed with deionized water and was dried in a vacuum oven for 1.5 h before weighing.

Reagent grade cupric sulfate and sulfuric acid were used to prepare the plating bath. Preliminary experiments showed that dissolved oxygen in the electrolyte could greatly affect the accuracy of current efficiency measurement as shown in Table 1. With high concentrations of sulfuric acid, dissolved oxygen tends to oxidize the deposit, resulting in a current efficiency seemingly larger than 100%. With nitrogen purge and a decreased concentration of sulfuric acid, a current efficiency close to 100% was obtained under d.c. Thus, in the following pulse current experiments, the composition was 0.2 M $CuSO_4 \cdot 5H_2O$ and 0.45 M H_2SO_4. Nitrogen was purged for at least 2 h and a nitrogen atmosphere was maintained during the electrodeposition. The plating bath was controlled at 25 °C and was magnetically stirred at 300 rpm.

The pulse current was generated from a potentiostat/galvanostat (EG&G PARC, model 362) which was controlled by a function generator (BNC Corp., model 625). The pulse period was controlled between 200 and 0.02 ms and the duty cycles between 0.5 and 0.2. The rise time for the applied current from the pulse generator was 2.5 ns. The potential responses were stored through an analog output unit of an interface card (UEI PD2-MF-16-50/16H) in a personal computer. The maximum speed of the interface card was 50 k data s^{-1}. To insure steady-state plating, the potential responses were stored after plating for 2 min.

3. Results and discussion

The reduction mechanism of copper has been studied in detail [19–27]. Chen and Wan [12] proposed a model for copper electrodeposition in the pulse plating, which could account for the decrease of current efficiency:

$$Cu^{2+}_{(aq)} \leftrightarrow Cu^{2+}_{(ad)} \quad \text{adsorption} \tag{1}$$

$$Cu^{2+}_{(ad)} + e^- \leftrightarrow Cu^{+}_{(ad)} \quad \text{first-step charge transfer} \tag{2}$$

$$Cu^{+}_{(ad)} + e^- \leftrightarrow Cu_{(ad)} \quad \text{second-step charge transfer} \tag{3}$$

$$Cu_{(ad)} \leftrightarrow Cu_{(cry)} \quad \text{surface diffusion} \tag{4}$$

$$2Cu^{+}_{(ad)} \leftrightarrow Cu^{2+}_{(aq)} + Cu_{(s)} \quad \text{disproportionation} \tag{5}$$

$$Cu_{(ad)} \leftrightarrow Cu_{(s)} \quad \text{dissolution} \tag{6}$$

The cupric ions are firstly adsorbed on the electrode and reduced to copper adatoms in two steps. Then the adatoms diffuse to steps and kink sites, where they are

incorporated into the metal matrix. However, two pathways may compete with the main process, giving a decrease in current efficiency in pulse plating. The first is the disproportionation reaction of cuprous ions, as shown in Equation 5; and the other is the dissolution of metal, as shown in Equation 6. During the off period, the cuprous ions may undergo disproportionation to form copper atoms and cupric ions which diffuse back into the bulk solution, naturally lowering the current efficiency for deposition. Alternatively, the adatoms may degrade as copper atoms suspended in the bulk solution and dissolve into the bulk solution by Equation 5, before they diffuse to kink sites, which also causes a reduction in current efficiency.

Current efficiencies of copper deposition with different pulse periods and duty cycles are shown in Figure 1. The pulse current density was controlled at 7.89 mA cm^{-2}, and the pulse periods at 200, 20, 2, 0.2 and 0.02 ms. Each current efficiency was measured from duplicate experiments. With the same pulse period, systems under 0.5 duty cycle have higher current efficiency than those under 0.2 duty cycle. This is reasonable since a 0.2 duty cycle means longer off-time than the 0.5 duty cycle, so more cuprous ions can undergo the disproportionation reaction in the former case. This result is consistent with Wan's study [11]. With a given duty cycle, current efficiency decreases with decreasing pulse period in the millisecond range and, surprisingly, increases with decreasing pulse period in the microsecond range. For instance, the current efficiency in the 0.2 duty cycle decreases from 87.7 to 82.9% when the pulse period changes from 200 to 2 ms. However, when the pulse period changes from 2 to 0.02 ms, the current efficiency actually increases from 82.9 to 94.3%. The decrease in current efficiency in the millisecond range has been explained by Chen and Wan [12] in terms of adatom dissolution. However, why current efficiency increases with shorter t_{on} in the microsecond pulse period range has never been explained. Since the double layer effect theoretically should become relatively more significant in the microsecond pulse than in the millisecond pulse, we attempted to study the double layer effect on the potential responses in order to explain why the current efficiency increases with shortening pulses in the microsecond range.

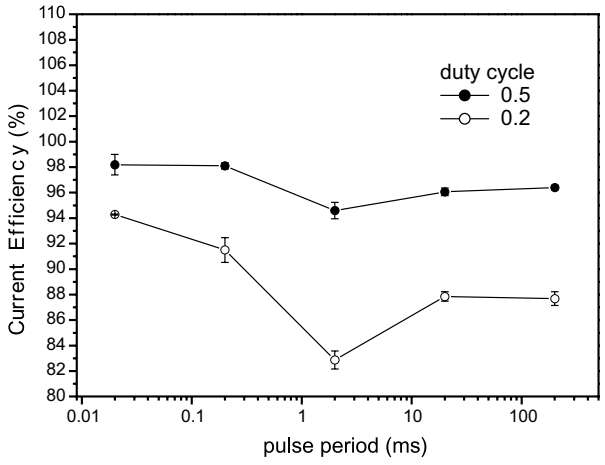

Fig. 1. Influence of pulse periods and duty cycles on current efficiency. Pulse current density 7.89 mA cm^{-2}. Pulse period: 200, 20, 2, 0.2 and 0.02 ms.

3.1. *Potential responses*

The rate-determining step for copper deposition at low current d.c. was identified to be charge transfer and surface diffusion [19]. An equivalent circuit model was proposed by Reid and David [26] for studying the impedance behaviour of a sulfuric acid–cupric sulfate/copper cathode interface. We found that pulse plating was theoretically similar to impedance analysis, and so adopted their concept in our developing model for pulse plating, including the double layer effect that cannot be neglected for very short pulses. The circuit model of the copper/electrolyte interface, applicable to pulse current plating at low current density, is shown in Figure 2, where R_{sol} is the resistance of the electrode solution, R_{ct} is the resistance of the first-step charge transfer (Equation 2), C_{dl} is the capacitance of the double layer, R_{sd} is the resistance of the second-step charge transfer and surface diffusion (Equations 3 and 4) and C_{psd} is the corresponding pseudocapacitance.

The pulse current density, i_p, in Section 1 is divided into the capacitive current density, i_C, and the faradaic current density, i_F. Their relation is as follows:

$$i_C + i_F = i_p \tag{7}$$

The capacitive current density is related to the potential by Equation 8:

$$i_C = C_{dl}\frac{d\eta^I}{dt} \tag{8}$$

where η^I is the potential drop corresponding to Equation 2 and C_{dl} is the capacitance of double layer which is independent of η^I.

Since the applied current density is low, the relationship between faradaic current and overpotential can be assumed linear and the faradaic current density can be written as

$$i_F = \frac{1}{R_{ct}}\eta^I \tag{9}$$

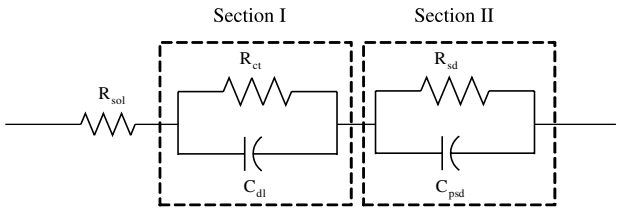

Fig. 2. Equivalent circuit of a pulse plating system.

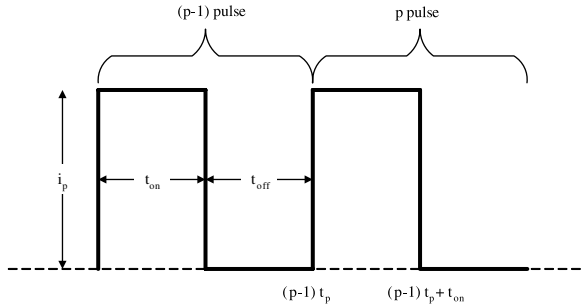

Fig. 3. Schematic diagram of pulse current waveform.

Substituting Equations 8 and 9 into Equation 7 produces Equation 10:

$$C_{dl}\frac{d\eta^{I}}{dt}+\frac{1}{R_{ct}}\eta^{I}=i_{p} \tag{10}$$

Since i_p is a step function, as shown in Figure 3, the response of η^I can be solved from Equation 10 and its initial condition, where p is the pulse number and t_p is the pulse period defined as $t_p = t_{on} + t_{off}$. During the ON period, the initial condition of Equation 10 at the beginning of the ON period is

$$\eta^{I}=\eta^{I}_{(p-1)t_p} \quad \text{at} \quad t=(p-1)t_p \tag{11}$$

Thus, Equations 10 and 11 can describe the response of η^I during the ON period:

$$\eta^{I}=i_pR_{ct}-\left(i_pR_{ct}-\eta^{I}_{(p-1)t_p}\right)\times\exp\left[-\left(t-(p-1)t_p\right)/R_{ct}C_{dl}\right]. \tag{12}$$

During the OFF period, the initial condition of Equation 10 at the beginning of the OFF period is

$$\eta^{I}=\eta^{I}_{(p-1)t_p+t_{on}} \quad \text{at} \quad t=(p-1)t_p+t_{on} \tag{13}$$

So again the solution of Equation 10 provides the response of η^I during the OFF period

$$\eta^{I}=\eta^{I}_{(p-1)t_p+t_{on}}\exp\left[-\left(t-(p-1)t_p-t_{on}\right)/R_{ct}C_{dl}\right] \tag{14}$$

Similar to η^I, the response of the potential drop corresponding to Equations 3 and 4 during the ON period is η^{II}, and

$$\eta^{II}=i_pR_{sd}-\left(i_pR_{sd}-\eta^{II}_{(p-1)t_p}\right)\times\exp\left[-\left(t-(p-1)t_p\right)/R_{sd}C_{psd}\right] \tag{15}$$

During the OFF period, the response of η^{II} is

$$\eta^{II}=\eta^{II}_{(p-1)t_p+t_{on}}\exp\left[-\left(t-(p-1)t_p-t_{on}\right)/R_{sd}C_{psd}\right] \tag{16}$$

So the total surface overpotential, η, is related to η^I and η^{II} as follows:

$$\eta=\eta^{I}+\eta^{II} \tag{17}$$

Hence, the response of electrode potential measured against the reference electrode is

$$E=E_{eq}+i_pR_{sol}+\eta \tag{18}$$

where E_{eq} is the equilibrium potential between the working electrode and the reference electrode, which is equal to the open circuit potential, and i_pR_{sol} is the ohmic overpotential. Because the pulse current density is very low, the concentration overpotential is neglected.

With high solution concentration, double layer capacitance is generally considered independent of potential [27]. Kelly and West [28] suggested that the double layer capacitance is independent of potential and frequency when simulating the impedance of copper deposition. In this study, the solution composition is 0.2 M $CuSO_4 \cdot 5H_2O$ and 0.45 M H_2SO_4, which is a concentrated solution. Hence, C_{dl} and C_{psd} are independent of potential and frequency in this model. C_{dl} depends on frequency only at low concentration [29, 30]. Tantavichet and Pritzker [30] proposed that the double layer capacitance depends on frequency and potential in the simulation of potential response for high frequency galvanostatic pulses. Their case is in the low-concentration region.

The experimental and simulated potential responses with various pulse periods are shown in Figures 4 and 5. Due to the limitation of the interface card, the potential response of 0.02 ms pulse was too fast to be detected. The simulated lines were produced by using the parameters in Table 2 which were chosen to fit the responses from the experiment. The simulation in general matches the experimental result. The double layer capacitance chosen was 50 μF cm^{-2}, which agrees well with the result of Kelly and West [28], which indicates the model is reasonable. The pseudocapacitance chosen was 500 μF cm^{-2}, which differs very much from the impedance study of Reid and David [26]. The pseudocapacitance is physically associated with the second-step charge transfer and the surface diffusion. Since only a small a.c. amplitude was applied in the impedance study, the surface diffusion was naturally quite different from that in the pulse plating. Hence, the pseudocapacitance used in the simulation differs from the results of the impedance measurements.

Figures 6 and 7 shows the simulated responses of η, η^I and η^{II} with different pulse periods and at 0.5 or 0.2 duty cycle. In the case of 200 ms t_p, both η^I and η^{II} contribute to η, indicating that charge transfer and surface diffusion are both rate-determining steps. When the pulse period was shortened, the contribution of η^{II} decreases and the contribution of η^I increases because the time constant $R_{ct}C_{dl}$ is smaller than $R_{sd}C_{psd}$. In the case of 0.2 ms t_p, η is dominated by η^I, indicating that the first-step charge transfer is the rate-determining step of the

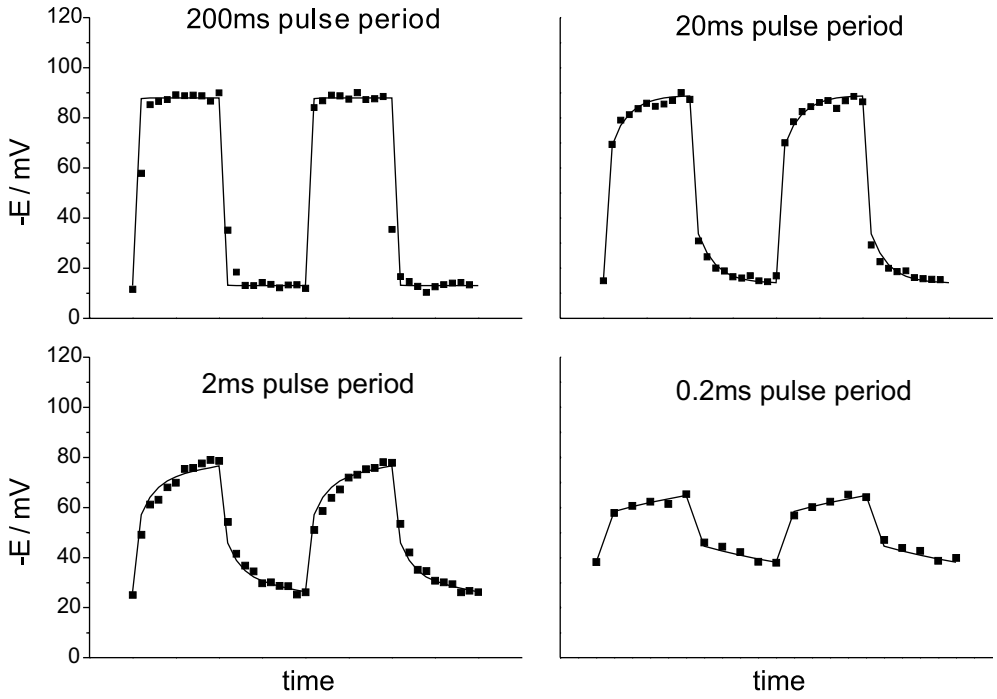

Fig. 4. Experimental and simulated potential responses with different pulse periods of 0.5 duty cycle.

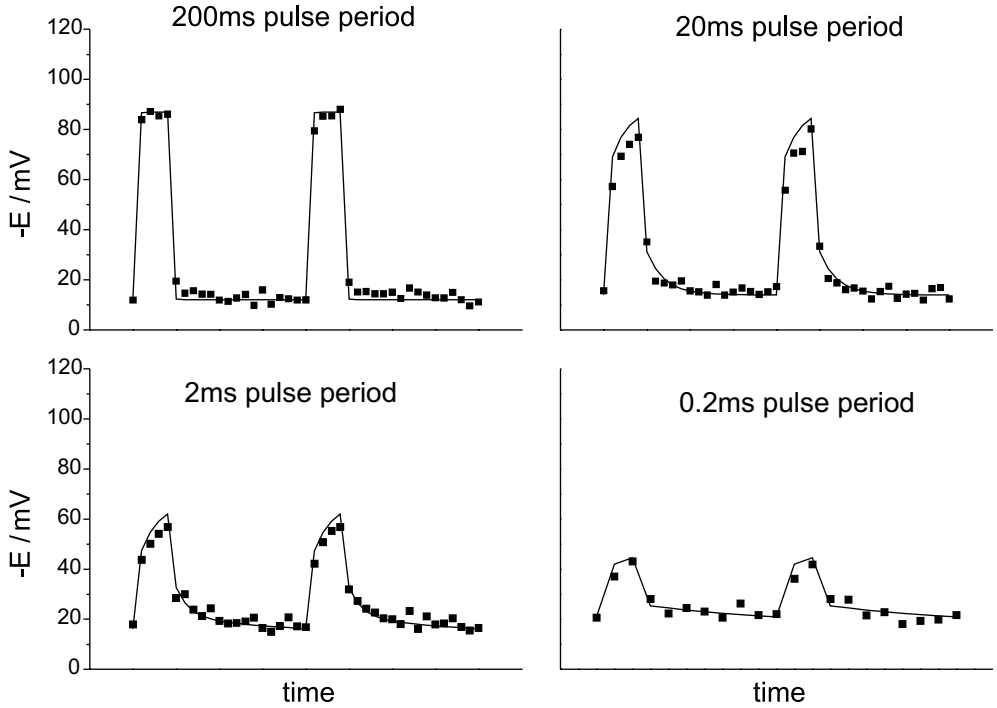

Fig. 5. Experimental and simulated potential responses with different pulse periods of 0.2 duty cycle.

overall reaction. This result is consistent with Reid and David [26]. They found that the rate-determining step of impedance at high frequency is the first-step charge transfer and at low frequency is surface diffusion.

3.2. *The mechanism of copper electrodeposition*

From the above results related to current efficiency and the potential responses, we postulated a mechanism of copper electrodeposition under pulse current. As shown in Figure 1, the current efficiency decreases with decreasing pulse period in the millisecond region, and the current efficiency increases with decreasing pulse period in the microsecond region. From the simulated responses of η shown in Figures 6 and 7, surface overpotential decreases with decreasing pulse period due to charging and discharging the double layer. Table 3 shows the surface overpotential at the end of the ON period with

Table 2. Parameters used in the simulation of potential response

Parameter	Value
Resistance of electrolytic solution, R_{sol}*	2.3 Ω cm^2
Resistance of first-step charge transfer, R_{ct}	3.1 Ω cm^2
Double layer capacitance, C_{dl}	50 μF cm^{-2}
Resistance of second-step charge transfer and surface diffusion, R_{sd}	4.1 Ω cm^2
Pseudocapacitance, C_{psd}	500 μF cm^{-2}
Equilibrium potential, E_{eq}	−10 mV

* R_{sol} was determined at 25 °C by the measurement of solution conductivity using a WTW LF 539 microprocessor conductivity meter.

different pulse periods and duty cycles. In the millisecond range, charge transfer and surface diffusion are the rate-determining steps. The adatoms, $Cu_{(ad)}$, are incorporated into steps and kink sites by surface diffusion, then the adatoms are likely to dissolve into the bulk solution at low surface overpotential in a surface diffusion controlled system. Since the surface overpotential decreases with decreasing pulse period, the current efficiency consequently decreases with shorter pulse period in the millisecond pulse period.

However, when we shorten the pulse period into the microsecond range, the response of η is dominated by η^{I} due to the smaller $R_{ct}C_{dl}$ time constant. The first-step charge transfer is the only rate-determining step of the overall reaction. Most adatoms may quickly be incorporated into steps and kink sites and there is little chance for the adatoms to undergo Equation 6 during the surface diffusion with those very short pulses. In fact, the shorter the pulse, the more complete is the incorporation. Thus, although the surface overpotential is still low, the current efficiency increases with decreasing pulse period. In addition, cuprous ions have insufficient time to undergo disproportionation during the microsecond pulses, which also leads to increase in current efficiency.

To further confirm this mechanism, we compare the current efficiency of the 0.02 ms pulse current with different duty cycles (0.5, 0.2 and 0.1 duty cycles) and its corresponding d.c. cases. These results are shown in Table 4, indicating that the current efficiency of the 0.02 ms pulse current with different duty cycles is actually higher than that of its corresponding d.c. case. For instance, the average current density of the '0.2 duty cycle pulse' is 1.58 mA cm^{-2}, and the current efficiency is 94.3%. However, the current efficiency of 1.58 mA cm^{-2} d.c. is 92.0%. For the d.c. system, the surface overpotential was measured to be 12.4 mV. The adatoms are incorporated into steps and kink sites by surface diffusion and dissolve more easily into the bulk solution at such low surface overpotential since the copper adatoms are able to go through Equation 6 in a surface diffusion controlled system. For the '0.2 duty-cycle pulse' with 0.2 ms pulses, the surface overpotential is about 14.4 mV from Table 3. The surface overpotential of the '0.2 duty cycle pulse' with 0.02 ms pulses must be lower than 14.4 mV. However, in pulse plating with 0.02 ms t_p, most adatoms are directly incorporated into steps and kink sites, and have less chance to undergo the dissolution process (Equation 6) since surface diffusion is no longer the controlling step. Hence, the current efficiency for pulse current in the microsecond range is higher than that of its corresponding d.c. case. However, this does not mean that dissolution does not exist in

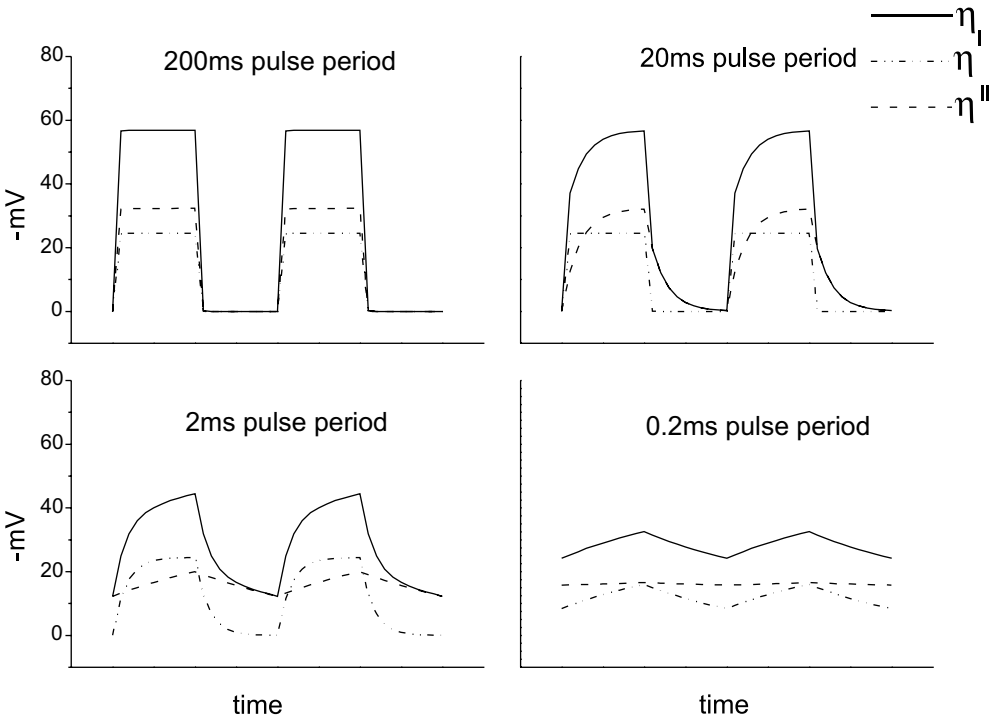

Fig. 6. Simulated responses of η, η^{I} and η^{II} at 0.5 duty cycle.

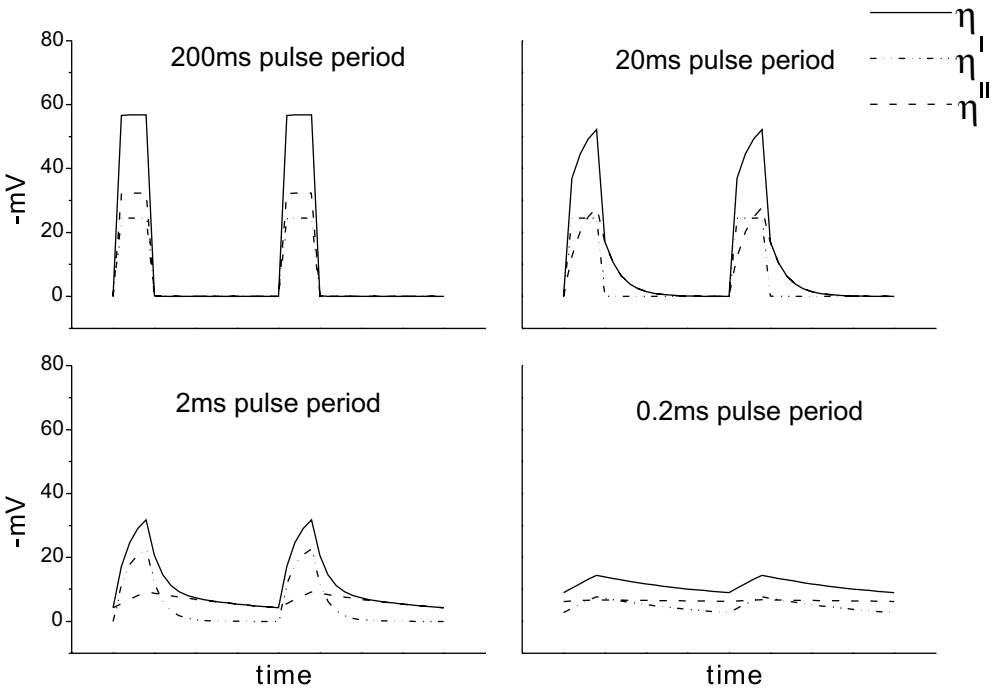

Fig. 7. Simulated responses of η, η^{I} and η^{II} at 0.2 duty cycle.

Table 3. Surface overpotential at the end of ON period with different pulse periods and duty cycles

Pulse period /ms	0.5 duty cycle Surface overpotential/mV	0.2 duty cycle Surface overpotential/mV
200	−56.8	−56.8
20	−56.6	−52.2
2	−44.5	−31.8
0.2	−32.6	−14.4

pulse plating. As shown in Table 4, the continuous decrease in current efficiency, as current density is reduced under either pulse current or d.c., is primarily due to the dissolution of $Cu_{(ad),}$ which becomes more pronounced as the applied current is reduced.

Theoretically, then, purely based on current efficiency, microsecond-range pulse plating can provide higher current efficiency than either d.c. or pulse plating in the millisecond range.

4. Conclusions

With pulses in the millisecond range, charge transfer and surface diffusion are the rate-determining steps. Shortening the pulse period in the microsecond range changes the rate-determining step from charge transfer and surface diffusion to the first-step charge transfer.

The reduction of cupric ions to copper adatoms can be adversely affected by the disproportionation of cuprous ions and the dissolution of copper adatoms into bulk solution. These two factors mainly account for the decrease in current efficiency in the millisecond-range pulse current in a surface diffusion controlled system. However, in the microsecond range, the adatoms are directly incorporated into steps and kink sites since surface diffusion is no longer the controlling step. The disproportionation of cuprous ions or the dissolution of copper adatoms has less chance to occur with very short t_p. Hence the current efficiency increases with decreasing pulse period in the microsecond range.

Table 4. Current efficiency of the 0.02 ms pulse current with different duty cycles and results from corresponding d.c. cases

Pulse duty cycle	Average current density* /mA cm^{-2}	Current efficiency /%			Average
0.5	3.95	98.8	97.6		98.2
0.2	1.58	94.3	94.3		94.3
0.1	0.789	72.0	79.8	76.0	75.9
	Corresponding current density /mA cm^{-2}	Current efficiency /%			Average
DC	3.95	96.7	94.9		95.8
	1.58	91.7	92.2		92.0
	0.789	70.6	68.9		69.8

* Average current density of pulse current is defined as $i_{avg} = i_p \times$ duty cycle, where $i_p = 7.89$ mA cm^{-2}.

In practice, if current efficiency is an important factor in certain copper pulse plating processes, then it is clear that there is a minimum current efficiency regarding the length of pulse period.

References

1. J.M. Quemper, E.D. Gergam, N.F. Rodriquez, J.P. Gilles, J.P. Grandchamp and A. Bosseboeuf, *J. Micromech. Microeng.* **10** (2000) 116.
2. N.S. Qu, K.C. Chan and D. Zhu, *Surf. Coat. Technol.* **91** (1997) 220.
3. J.J. Kelly, P.E. Bradley and D. Landolt, *J. Electrochem. Soc.* **147** (2000) 2975.
4. E.T. Taylor, J.J Sun and M.E. Inman, *Plat. Surf. Finish.* **87** (2000) 68.
5. C. Lingk and M.E. Gross, *J. Appl. Phys.* **84** (1998) 5547.
6. H.Y. Cheh, *J. Electrochem. Soc.* **118** (1971) 1132.
7. K. Viswanathan and H.Y. Cheh, *J. Electrochem. Soc.* **126** (1979) 398.
8. D-T. Chin, *J. Electrochem. Soc.* **135** (1983) 1657.
9. A.C. West, C.C. Cheng and B.C. Baker, *J. Electrochem. Soc.* **145** (1998) 3070.
10. C.C. Wan, H.Y. Cheh and H.B. Linford, *Plat. Surf. Finish.* **63** (1977) 66.
11. C.C. Wan, H.Y. Cheh and H.B. Linford, *J. Appl. Electrochem.* **9** (1979) 29.
12. C.J. Chen and C.C. Wan, *J. Electrochem. Soc.* **136** (1989) 2850.
13. T.A. Eckler, B.A. Manty and P.L. Mcdaniel, *Plat. Surf. Finish.* **66** (1980) 60.
14. S. Yoshimura, S. Chida and E. Sato, *Met. Finish.* **84** (1986) 66.
15. K. Hosokawa, H. Angerer, J.Cl. Puippe and N. Ibl, *Plat. Surf. Finish.* **66** (1980) 52.
16. W.S. Miu and Y.S. Fung, *Plat. Surf. Finish.* **73** (1986) 66.
17. J. Cl. Puippe and N. Ibl, *J. Appl. Electrochem.* **10** (1980) 775.
18. W.C. Tsai, C.C. Wan and Y.Y. Wang, *J. Electrochem. Soc.* **149** (2002) C229.
19. E. Mattsson and J.O'M. Bockris, *Trans. Farad. Soc.* **55** (1959) 1586.
20. J.O'M. Bockris and H. Kita, *J. Electrochem. Soc.* **109** (1962) 928.
21. O.R. Brown and H.R. Thirsk, *Electrochimi. Acta* **10** (1965) 383.
22. G.W. Tindall and S. Bruckenstein, *Anal. Chem.* **40** (1968) 1051.
23. W.J. Lorenz, H.D. Hermann, N. Wüthrich and F. Hilbert, *J. Electrochem. Soc.* **121** (1974) 1167.
24. J.R. White, *J. Appl. Electrochem.* **17** (1987) 977.
25. E. Gileadi and V. Tsionsky, *J. Electrochem. Soc.* **147** (2000) 567.
26. J.D. Reid and A.P. David, *J. Electrochem. Soc.* **134** (1987) 1389.
27. M. Paunovic and M. Schlesinger, 'Fundamentals of Electrochemical Deposition' (John Wiley & Sons, New York, 1998), p. 103.
28. J.J. Kelly and A.C. West, *J. Electrochem. Soc.* **145** (1998) 3477.
29. J.O'M. Bockris and B.E. Conway, *J. Chem. Phys.* **28** (1958) 707.
30. N. Tantavichet and M.D. Pritzker, *J. Electrochem. Soc.* **149** (2002) C289.